AIP Applied Physics Letters

Relationship between Gilbert damping and magneto-crystalline anisotropy in a Ti-buffered Co/Ni multilayer system

Hyon-Seok Song, Kyeong-Dong Lee, Jeong-Woo Sohn, See-Hun Yang, Stuart S. P. Parkin et al.

Citation: Appl. Phys. Lett. **103**, 022406 (2013); doi: 10.1063/1.4813542
View online: http://dx.doi.org/10.1063/1.4813542
View Table of Contents: http://apl.aip.org/resource/1/APPLAB/v103/i2
Published by the AIP Publishing LLC.

APPLIED PHYSICS LETTERS **103**, 022406 (2013)

Relationship between Gilbert damping and magneto-crystalline anisotropy in a Ti-buffered Co/Ni multilayer system

Hyon-Seok Song,[1,2] Kyeong-Dong Lee,[1,3] Jeong-Woo Sohn,[1,2] See-Hun Yang,[4] Stuart S. P. Parkin,[4] Chun-Yeol You,[5] and Sung-Chul Shin[1,2,a)]

[1]*Department of Physics and Center for Nanospinics of Spintronic Materials, Korea Advanced Institute of Science and Technology, Daejeon 305-701, South Korea*
[2]*Department of Emerging Materials Science, DGIST, Daegu 711-873, South Korea*
[3]*Department of Materials Science and Engineering, KAIST, Daejeon, 305-701, South Korea*
[4]*IBM Research Division, Almaden Research Center, San Jose, California 95120, USA*
[5]*Department of Physics, Inha University, Incheon 402-751, South Korea*

(Received 19 March 2013; accepted 21 June 2013; published online 9 July 2013)

The relationship between Gilbert damping and magneto-crystalline anisotropy is studied here using an all-optical method in a perpendicular Co/Ni multilayer system by varying the Ti-buffer thickness. As the Ti-buffer thickness increases, the magneto-crystalline anisotropy is enhanced. The time-resolved Kerr signal of each sample is well described by its own intrinsic Gilbert damping constant in a wide range of the external magnetic field. Interestingly, we find that Gilbert damping constants increase linearly from 0.021 to 0.036 when the magneto-crystalline anisotropy of the samples varies from 2.4 to 3.4 Merg/cm^3. Such a linear relationship implies that the spin-orbit interaction is the main source of the damping process through spin-lattice relaxation in our system. © *2013 AIP Publishing LLC*. [http://dx.doi.org/10.1063/1.4813542]

In recent years, there has been growing interest in spin-transfer torque magnetic random access memory (STT-MRAM). To enable dense memory architectures, lowering the critical switching current density J_c is essential. In addition, to create thermally stable memory architectures, increasing the magnetic anisotropy is important. It is well known that J_c varies in proportion to the Gilbert damping constant α.[1] Therefore, it is crucial to understand and control both α and the magnetic anisotropy to realize STT-MRAM.

Many theoretical studies have been carried out in an effort to understand the origin of Gilbert damping. The Gilbert damping can be classified into local and non-local damping according to the dissipation location.[2] With local damping, the spin energy is transferred to the lattice via spin-orbit coupling and magnon scattering within the ferromagnetic layer.[3] In contrast, at the interface between the ferromagnetic layer and the nonmagnetic layer, non-local damping, particularly spin-pumping, occurs when the spin energy of the ferromagnetic layer dissipates through the interface into normal metals via spin current or spin waves.

Among these origins of damping, spin-orbit coupling is closely related to perpendicular magnetic anisotropy (PMA) from magneto-crystalline anisotropy.[4] Because PMA and α are very important for the realization of STT-MRAM, the relationship between two is now an emerging issue.[5–11] Silva *et al.*[9] showed that the spin density, rather than PMA, critically affects α in $Co_{90}Fe_{10}$/Ni multilayers and alloys. On the other hand, some reports have shown that PMA is related to α when spin pumping exists in Pt/Co/Pt, Co/Pd multilayer and FePdPt films.[5,6,12] In another respect, in iron-rich $Fe_{1-x}Si_x$ without spin pumping,[13] magneto-crystalline anisotropy showed a nonlinear relationship to α. In this case, the Si concentration affects not only the electronic structure but also the total magnetic moment. Therefore, the relationship among α, the spin density, spin pumping, and magneto-crystalline anisotropy remains unclear.

To clarify this, we explore a more direct relationship between α and the magneto-crystalline anisotropy in a Ti-buffered Co/Ni multilayer system, in which spin pumping is negligible and where the total magnetic moment is almost same. For this purpose, we change the magneto-crystalline anisotropy of the Co/Ni multilayer system by varying only the Ti-buffer layer thickness d_{Ti} from 1.5 to 9 nm. The Ti-buffer layer is also crucial when intending to exclude the spin-pumping effect. In addition, we used multilayer with stack number $N = 6$, facilitating nearly homogeneous perpendicular magnetic anisotropy and thereby minimizing the inhomogeneity effect. Multilayer films of Ti(d_{Ti} nm)/Co(0.3 nm)/[Ni(0.7 nm)/Co(0.15 nm)]$_6$/TaN(5 nm) were grown by DC magnetron sputtering on Si/SiO_2 (001) substrates. With the polar magneto-optical Kerr effect (p-MOKE) and an in-plane vibrating sample magnetometer (VSM), we measured the static magnetic properties. The improvement of the crystallinity was checked by X-ray measurements. Figure 1(a) shows the polar magneto-hysteresis loops of the samples by using p-MOKE. All samples show very square loops, indicating PMA of the sample. As shown in Fig. 1(b), the measured magnetic coercivity H_c increases as the Ti-buffer layer thickness increases. From the in-plane magneto-hysteresis loop, we measured the saturation magnetic field H_s and estimated the uniaxial magnetic anisotropy K_u using the simple equation $K_u = M_s H_s/2 + 2\pi M_s^2$, where M_s is the saturation magnetization. Figure 1(c) shows K_u as a function of d_{Ti}. The increase of K_u (ΔK_u) indicates that the crystallinity enhancement due to the better buffer layer morphology increases the magneto-crystalline anisotropy.[14,15]

The Gilbert damping constant is characterized by means of time-resolved magneto-optical Kerr effect (TR-MOKE)

a)Electronic addresses: shin@kaist.ac.kr and scshin@dgist.ac.kr

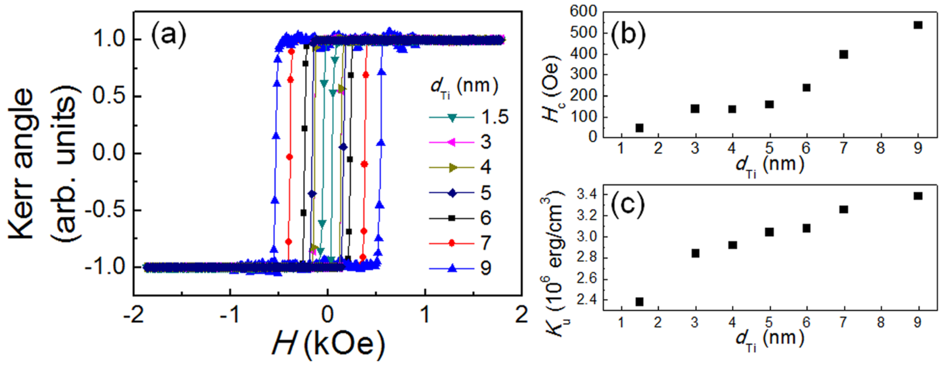

FIG. 1. (a) Magnetic hysteresis loop measured by p-MOKE with Ti-buffer layer thickness, $d_{\mathrm{Ti}} = 1.5 \sim 9$ nm. (b) Coercivity field H_c as a function of d_{Ti}, which is measured by p-MOKE. (c) Uniaxial magnetic anisotropy K_u as a function of d_{Ti}.

measurement. A schematic of the TR-MOKE setup is shown in Fig. 2(a). The sample is excited by a 800-nm pump beam, and its fluence is approximately 8.15 mJ/cm^2. The probe beam fluence is much weaker than the pump beam fluence F. We checked out that the transient heating and cooling by the pump beam is negligible in precessional time regime (>50 ps).[11] The heated-up temperature and its dynamics of our ferromagnetic layer are in good agreement with previous reports.[16,17] Pump and probe laser pulses are fed into a $50\times$(0.5 numerical aperture) polarization-conserving objective lens. The probe beam reflects onto the normal axis of a sample. The polar Kerr signal is measured using a balanced detection technique. The applied external magnetic field H ranges from 3.5 to 5.3 kOe with an angle θ_H of 60° from the normal direction of the sample.[11,18]

The time-dependent Kerr signals, which are measured at a high magnetic field of $H = 5.3$ kOe, are shown in Fig. 2(b) for the [Co/Ni]$_6$ multilayer with d_{Ti} of 1.5, 3, 4, 5, 6, 7, and 9 nm. The signals are subtracted by the background signal with an exponential decay function, and the remaining precessional components θ_K are fitted with the damped harmonic function, $\theta_K = A\sin(2\pi f t + \varphi)\exp(-t/\tau)$, with tuning factors of φ and A, as shown by the solid curves in Fig. 2(b). Here, we can obtain the resonance frequency f and the relaxation time τ.

The representative data of f and τ^{-1} are shown in Figs. 3(a) and 3(b) in a wide range of H with the samples of $d_{\mathrm{Ti}} = 1.5$ and 9 nm, which have the lowest and the highest magneto-crystalline anisotropy in our sample series, respectively. The value of f increases with H, which is explained well by the

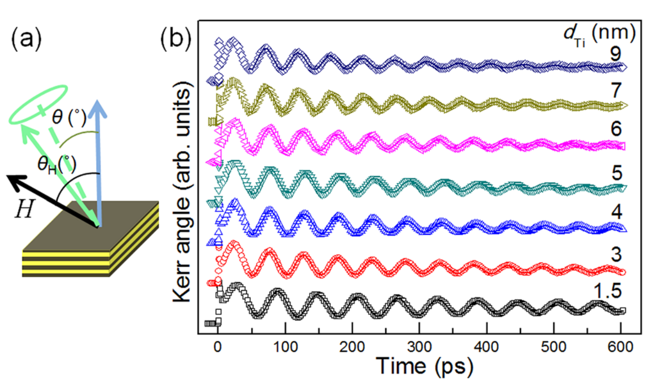

FIG. 2. (a) Schematic of experimental setup. (b) Time-resolved Kerr signals are measured with [Co/Ni]$_6$ multilayer films of $d_{\mathrm{Ti}} = 1.5 \sim 9$ nm at $H = 5.3$ kOe. The signals are shown in open symbols, and their fitted curves are shown in solid curves.

Kittel formula, $f = (\gamma/2\pi)\sqrt{H_1 H_2}$ with $H_1 = H\cos(\theta_H - \theta) + H_k^{\mathrm{eff}}\cos^2\theta$ and $H_2 = H\cos(\theta_H - \theta) + H_k^{\mathrm{eff}}\cos 2\theta$. Here, γ is the gyromagnetic ratio, which is defined as $\gamma = g\mu_B/\hbar$. The fitting parameter H_k^{eff} is the effective anisotropy field.[7] The equilibrium angle θ is determined from the energy-minimized relationship, $\sin 2\theta = 2H/H_k^{\mathrm{eff}}\sin(\theta_H - \theta)$. With the γ value of bulk Co, 19.4 Mrad/s·Oe ($g = 2.2$),[19] the best fitted values of H_k^{eff} are 1600 ± 300 and 4100 ± 100 Oe for multilayers with $d_{\mathrm{Ti}} = 1.5$ and 9 nm, respectively. These H_k^{eff} values are slightly smaller compared to those from the VSM measurement.

Figure 3(b) clearly shows that τ^{-1} is well fitted with the equation $\tau^{-1} = \gamma\alpha_{\mathrm{fit}}(H_1 + H_2)/2$. Because this relationship only holds for the intrinsic damping constant, it must be emphasized that the extrinsic damping process due to the inhomogeneity is negligible in our measurement. Therefore, we can say that α_{fit} obtained from the linear fit of τ^{-1} is essentially the intrinsic α of the given sample. The experimental τ^{-1} data are well fitted with the single damping parameter, α_{fit}, with values of 0.021 ± 0.001 and 0.036 ± 0.001 for $d_{\mathrm{Ti}} = 1.5$ and 9 nm, respectively.

The Gilbert damping constant α is investigated as a function of the Ti-buffer layer thickness d_{Ti} in Fig. 4(a). If the applied external magnetic field is strong enough, we can obtain α using the simple relationship of $\alpha = (2\pi f\tau)^{-1}$,[20] which show the same values as α_{fit} when $d_{\mathrm{Ti}} = 1.5$ and 9 nm. Here, f and τ are measured at 5.3 kOe, which is near or above the saturation magnetic field of the samples. We found that α increases with an increase in the Ti-buffer layer thickness. Similarly, we plotted α as a function of K_u in Fig. 4(b). Interestingly, we noted a linear correlation between K_u and α. The slope of 1.43×10^{-8} cm^3/erg in the Co/Ni multilayer system is about three times lower than that of 4.33×10^{-8} cm^3/erg in the Co/Pd multilayer system.[6] We assumed that this difference comes from negligible spin pumping effect in our Co/Ni multilayer system compared to the effect in the Co/Pd system.

Several possible causes of the increase of α with K_u can be imagined. One is non-local spin-current damping, which is caused by the precessing moment in an adjacent non-magnetic layer.[3] However, the spin-orbit coupling constant of Ti is more than 10 times weaker than that of Pd or Pt. Additionally, we checked out that spin pumping effect is negligible with $d_{\mathrm{Ti}} = 5$ nm in our Co/Ni multilayers.[11] Therefore, we believe that the non-local spin-current damping can be ignored. The second possibility is the multi-domain or inhomogeneity effect, which induces additional spin wave damping, as usually observed in the case of a large anisotropy distribution. However, in our

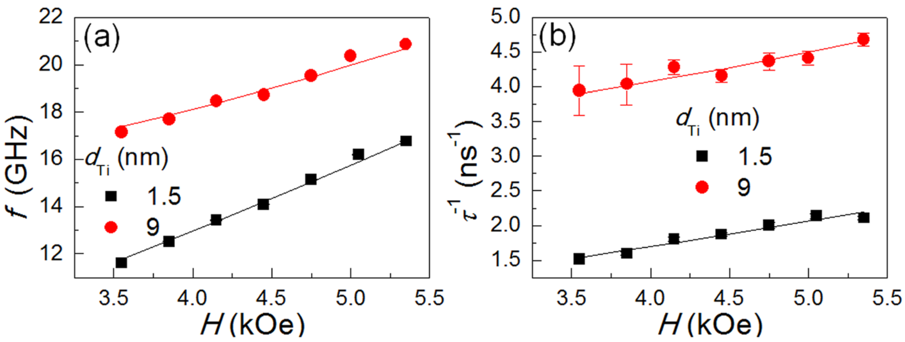

FIG. 3. Experimental data (solid symbols) and fitting curves (solid curves) of (a) the resonance frequency f and (b) the inverse of the relaxation time τ^{-1} as a function of the external magnetic field H.

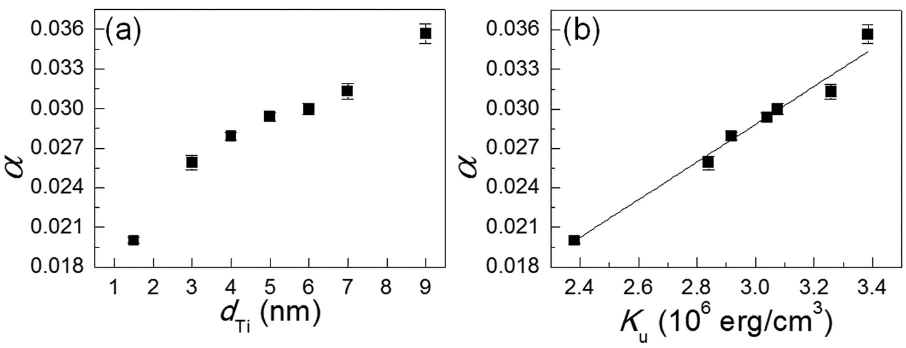

FIG. 4. (a) The α dependence on the Ti-buffer layer thickness and (b) the uniaxial magnetic anisotropy K_u at $H = 5.3$ kOe. The solid line is a linear fit.

experimental condition involving an external magnetic field strong enough to saturate a sample, this effect can be excluded.[3] Furthermore, as shown in Fig. 3(b), τ^{-1} is well fitted by a single damping parameter of each sample, guaranteeing that the extrinsic damping from the multi-domain or inhomogeneity effect is negligible. The third possibility is a thermal effect caused by the different Ti-buffer layer thickness. The thick Ti-buffer layer acts as a larger heat sink, resulting in a slightly lower equilibrium temperature of the ferromagnetic Co/Ni layers. However, above room temperature, α of Co and Ni is expected to increase slightly due to the phonon-assisted spin-orbit effect.[21] This indicates that the thermal effect of the Ti-buffer layer can reduce α in a thicker sample. The variation of α of our data is large, and the slope with respect to the Ti-buffer layer thickness is opposite to that of the thermal effect. Hence, we rule out this possibility. The fourth possibility is the interface roughness effect. The thickness of the buffer layer might affect the interface roughness. The dependence of the degree of damping on the roughness can be understood by considering the effects of the roughness-coupled eddy current.[22] Nevertheless, a recent study of a Co/Ni multilayer with a Cu buffer layer showed that α is less affected by the roughness.[23] The last possibility is that α becomes large in materials with high magneto-crystalline anisotropy because both α and the magneto-crystalline anisotropy are related somewhat by the spin-orbit coupling strength ξ. It has been long thought that one source of α may stem from the spin-orbit coupling.[24] Kamberský showed that α is also proportional to ξ^2.[25] On the other hand, Bruno showed that K_u arising from the magneto-crystalline anisotropy is roughly proportional to ξ^2 by estimation.[4] Therefore, our linear relationship between the magneto-crystalline anisotropy and α is clear evidence of their proportionality to ξ^2.

In conclusion, we investigate the relationship between Gilbert damping and magneto-crystalline anisotropy using TR-MOKE in the Co/Ni multilayer system by varying the Ti-buffer layer thickness. The Ti-buffer layer thickness changes the magneto-crystalline anisotropy by crystallinity enhancement and affects the Gilbert damping constant. We find that the magneto-crystalline anisotropy and the Gilbert damping constant show a linear relationship. This can be interpreted by the spin-orbit coupling, which is related to both the magneto-crystalline anisotropy and the Gilbert damping constant with the proportionality of ξ^2. This interrelationship emphasizes that magneto-crystalline anisotropy is one of main keys to control critical switching current density in realization of STT-MRAM.

This work was supported by the DGIST R&D Program of the Ministry of Education, Science and Technology of Korea (11-IT-01). It was also supported by a grant from the National Research Foundation of Korea (NRF) funded by the Korean government (MEST) (Grant Nos. NRF-2007-0056631, 2010-0023798, 2010-0022040, and 2012R1A1A1041590).

[1]D. Lacour, J. A. Katine, N. Smith, M. J. Carey, and J. R. Childress, Appl. Phys. Lett. **85**, 4681 (2004).
[2]M. D. Kaufmann, Ph.D. thesis, Georg-August-Universität Göttingen, 2006.
[3]J. Walowski, M. D. Kaufmann, B. Lenk, C. Hamann, J. McCord, and M. Münzenberg, J. Phys. D **41**, 164016 (2008).
[4]P. Bruno, *Physical Origins and Theoretical Models of Magnetic Anisotropy* (Ferienkurse des Forschungszentrums Jürich, Jürich, 1993).
[5]S. Mizukami, E. P. Sajitha, D. Watanabe, F. Wu, T. Miyazaki, H. Naganuma, M. Oogane, and Y. Ando, Appl. Phys. Lett. **96**, 152502 (2010).
[6]S. Pal, B. Rana, O. Hellwig, T. Thomson, and A. Barman, Appl. Phys. Lett. **98**, 082501 (2011).
[7]S. Mizukami, X. Zhang, T. Kubota, H. Naganuma, M. Oogane, Y. Ando, and T. Miyazaki, Appl. Phys. Express **4**, 013005 (2011).

[8]T. Kato, Y. Matsumoto, S. Okamoto, N. Kikuchi, O. Kitakami, N. Nishizawa, S. Tsunashima, and S. Iwata, IEEE Trans. Magn. **47**, 3036 (2011).
[9]J. M. Shaw, H. T. Nembach, and T. J. Silva, Appl. Phys. Lett. **99**, 012503 (2011).
[10]J. Shaw, H. Nembach, and T. Silva, Phys. Rev. B **85**, 054412 (2012).
[11]H.-S. Song, K.-D. Lee, J.-W. Sohn, S.-H. Yang, S. S. P. Parkin, C.-Y. You, and S.-C. Shin, Appl. Phys. Lett. **102**, 102401 (2013).
[12]P. He, X. Ma, W. Zhang, H. B. Zhao, G. Lüpke, Z. Shi, and S. M. Zhou1, Phys. Rev. Lett. **110**, 077203 (2013).
[13]I. Barsukov, S. Mankovsky, A. Rubacheva, R. Meckenstock, D. Spoddig, J. Lindner, N. Melnichak, B. Krumme, S. Makarov, H. Wende, H. Ebert, and M. Farle, Phys. Rev. B **84**, 180405 (2011).
[14]Q. Meng, P. de Haan, W. P. van Drent, J. C. Lodder, and T. J. A. Popma, IEEE Trans. Magn. **32**, 4064 (1996).
[15]Y. B. Zhang, J. A. Woollam, Z. S. Shan, J. X. Shen, and D. J. Sellmyer, IEEE Trans. Magn. **30**, 4440 (1994).
[16]E. Beaurepaire, J.-C. Merle, A. Daunois, and J.-Y. Bigot, Phys. Rev. Lett. **76**, 4250 (1996).
[17]J. Kisielewski, A. Kirilyuk, A. Stupakiewicz, A. Maziewski, A. Kimel, Th. Rasing, L. T. Baczewski, and A. Wawro, Phys. Rev. B **85**, 184429 (2012).
[18]K.-D. Lee, K.-S. Ryu, J.-W. Kim, H.-S. Song, J.-W. Jeong, and S.-C. Shin, Phys. Rev. B **82**, 140401(R) (2010).
[19]S. Chikazum, *Physics of Ferromagnetism* (Clarendon Press, Oxford, 1997).
[20]G. Malinowski, K. C. Kuiper, R. Lavrijsen, H. J. M. Swagten, and B. Koopmans, Appl. Phys. Lett. **94**, 102501 (2009).
[21]S. Bhagat and P. Lubitz, Phys. Rev. B **10**, 179 (1974).
[22]J. O. Rantschler, B. B. Mar, J. J. Mallett, P. Chen, R. D. McMichael, and W. F. Egelhoff, IEEE Trans. Magn. **41**, 3523 (2005).
[23]J. M. Shaw, H. T. Nembach, and T. J. Silva, J. Appl. Phys. **108**, 093922 (2010).
[24]M. Hickey and J. Moodera, Phys. Rev. Lett. **102**, 137601 (2009).
[25]V. Kamberský, Czech. J. Phys. **26**, 1366 (1976).